

000  
001  
002  
003  
004  
005  
006  
007  
008  
009  
010  
011  
012  
013  
014  
015  
016  
017  
018  
019  
020  
021  
022  
023  
024  
025  
026  
027  
028  
029  
030  
031  
032  
033  
034  
035  
036  
037  
038  
039  
040  
041  
042  
043  
044  
045  
046  
047  
048  
049  
050  
051  
052  
053

# Guided Proofreading of Automatic Segmentations for Connectomics

## *Supplemental Material*

Anonymous ICCV submission

Paper ID 0922

	Traditional Network		Residual Network	
Conv. Layers	2	4	5	13
Dropout Reg.	y	y	y	n
Cost [m]	27.5	383	5080	1094
Test. Acc.	0.925	0.94	0.93	0.90
Prec./Recall	0.93/0.93	0.94/0.94	0.7/0.53	0.74/0.66
F1 Score	0.93	0.94	0.39	0.64
		*		

Table 1: Traditional CNN Architecture versus Residual Network Architecture [1]. All configurations are compared using the same parameters. Our final choice (indicated by \*) trains relatively fast and performs better.

Parameter	Search Space
Filter size:	<b>3x3, 5x5, 9x9, 13x13</b>
No. Filters 1:	32, 48, <b>64</b>
No. Filters 2-4:	32, <b>48</b> , 64
Dense units:	256, <b>512</b>
Learning rate:	0.00001, 0.0001, 0.001, 0.01, <b>0.03-0.00001</b>
Momentum:	0.9, 0.95, <b>0.9-0.999</b>
Mini-Batchsize:	10, 100, <b>128</b>

Table 2: Brute force parameter search for the split error classifier. The final parameters are highlighted.

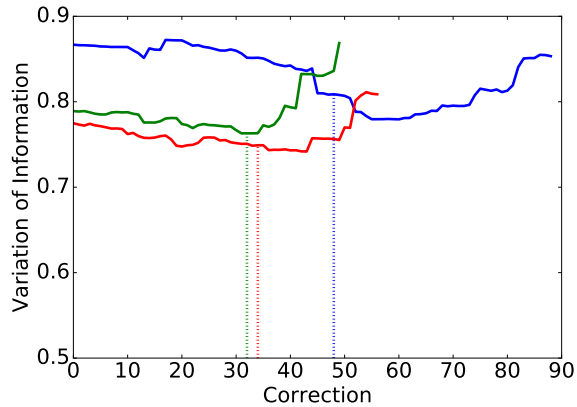


Figure 1: Observations of probability thresholds  $p_t$  during automatic selection on three different subvolumes of previously unseen testing data. The dashed lines show when  $p_t = 0.95$  is reached.

## 1. Classifier

### 1.1. Architecture

We explored different architectures for the convolutional neural network (CNN) for split error detection. We compare traditional CNN architectures versus residual networks [1] (Tab. 1). The traditional architecture with dropout regularization generalized better than residual networks on unseen testing data.

### 1.2. Training Parameters

We performed a limited brute force parameter search to tune the split error classifier (Tab. 2). This resulted in 3240 different CNN configurations which were evaluated on 10% of our training data. Learning rate and momentum ranges are defined linearly across 2000 epochs.

### 1.3. Automatic Method Threshold $p_t$

For automatic selection, we observed a threshold  $p_t = 0.95$  as stable when evaluating on previously unseen testing data (Mouse S1 AC3 Open Connectome Project dataset). This means that automatic selection stops once all borders with  $p_t \geq 0.95$  were proofread. Figure 1 shows split error

classification on three randomly selected subvolumes ( $700 \times 700 \times 2$  voxels) of AC3. In all cases, the threshold  $p_t = 0.95$  reduces VI.

108  
109  
110  
111  
112  
113  
114

#### 1.4. Merge Error Detection Pseudo Code

We provide pseudo code on how we detect merge errors to foster understanding of the reported algorithm (Alg. 1). In our experiments, we use  $N = 50$  iterations.

---

**Algorithm 1** Merge Error Detection for a label  $l$ 


---

```

1:  $l_d = \text{dilate}(l, 20)$ 
2:  $\text{invImage} = \text{invert}(\text{image})$ 
3: for N iterations do
4:    $s_1, s_2 = \text{randomSeedsOnBoundary}(l_d)$ 
5:    $\text{wsImage} = \text{watershed}(\text{invImage}, l_d, s_1, s_2)$ 
6:    $\text{border} = \text{border}(\text{wsImage})$ 
7:    $p = \text{rank}(\text{border})$ 
8:    $p_{\text{merge}} = 1 - p$ 
9: find(max  $p_{\text{merge}}$ )

```

---

#### 1.5. Limitations

Guided proofreading works on 2D image sections. This enables error correction without a computationally expensive alignment process. However, the output requires an additional (block-)merging step prior to 3D analysis. Several software packages exist for this purpose.

As described in Section 4, the guided proofreading classifier has to be retrained if used on a different species than mouse. In our experiments, parameters did not need to be changed.

## 2. Automatic Segmentation Pipeline

We create a dense automatic segmentation of electron microscopy data using a combination of a U-net [5] and the GALA agglomeration method [3]. To not bias, these classifiers are trained on different data than GP (Tab. 3).

Training Set U-Net / GALA	Training Set GP	Test Set GP
AC3+AC4 (1024 × 1024 × 175vx)	L. Cylinder (2048 × 2048 × 250vx)	L. Cylinder <sub>test</sub> (2048 × 2048 × 50vx)
AC4 excl. test (1024 × 1024 × 90vx)	L. Cylinder (2048 × 2048 × 250vx)	AC4 <sub>test</sub> subvolume (400 × 400 × 10vx)
AC3+AC4 (1024 × 1024 × 175vx)	CREMI A/B/C (1250 × 1250 × 300vx)	CREMI A/B/C <sub>test</sub> (1250 × 1250 × 15vx)

Table 3: Training data of membrane detection (U-Net / GALA) vs. training data of GP vs. test data.

GALA uses a random forest classifier to agglomerate segments. We use an agglomeration level of 0.3 (after a grid search). We follow the method by Knowles-Barley *et al.* as described in [2].

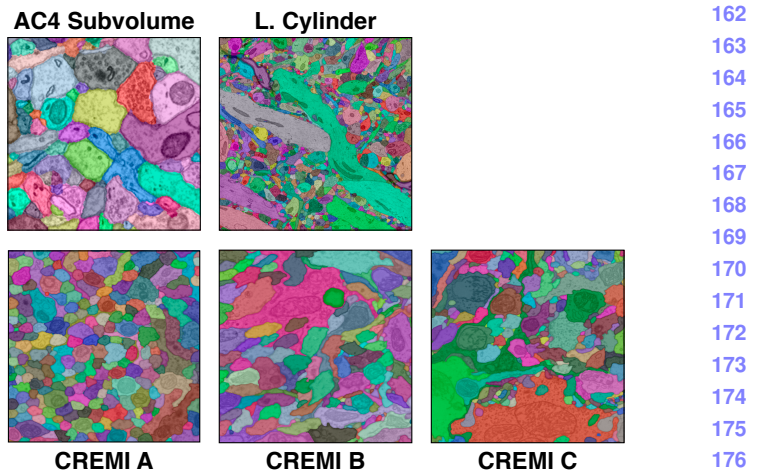


Figure 2: The five different datasets we use for evaluation. The top row shows the first slice of the AC4 and L. Cylinder mouse brain datasets as reported in the paper. The bottom row shows the first slice of the CREMI A/B/C fruit fly datasets which we used for additional experiments.

## 3. L. Cylinder Results

We report experiments and results on the L. Cylinder dataset in the paper. Figure 3 and 4 visualize the reported results measured as variation of information (VI). We compare automatic selection with threshold and selection oracle using focused proofreading and guided proofreading.

**Best possible VI.** The selection oracle using guided proofreading does not reach the best possible VI score. We calculate this score by intersecting the initial segmentation and the ground truth. In theory, the classifier should be able to reach this lower bound. However, due to the classification patch size, the membrane probability maps we used included a 30 pixel frame region. Guided proofreading ignores all segments within this frame region, and so cannot reach the best possible VI in some datasets.

## 4. Additional Experiments

**CREMI A/B/C.** As part of the MICCAI 2016 challenge on circuit reconstruction from electron microscopy images (CREMI), six ssTEM datasets were made publicly available<sup>1</sup>, each  $1250 \times 1250 \times 125$  voxels. Since only three datasets include manually-labeled ‘ground truth’, we use these three volumes for our experiments. The volumes are part of an adult fruit fly (*Drosophila melanogaster*) brain. The resolution of all three datasets is  $4 \times 4 \times 40 \text{ nm}^3/\text{voxel}$ . We evaluate error detection and correction on subvolumes of CREMI A/B/C with the dimensions  $1250 \times 1250 \times 5$

<sup>1</sup><http://www.creml.org>

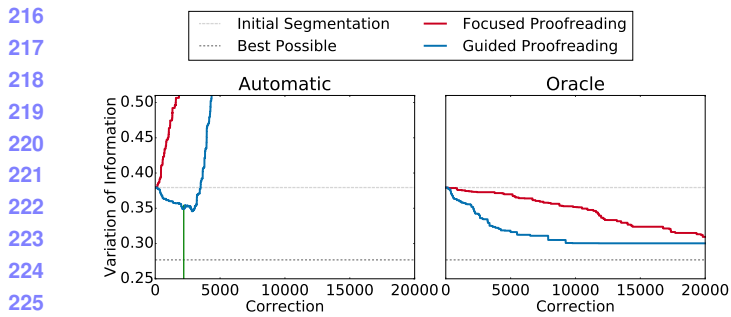


Figure 3: Performance comparison of Plaza’s focused proofreading and our guided proofreading on the L. Cylinder dataset as reported in the paper. All measurements are shown as median VI, the lower the better. We compare automatic selection with threshold ( $p_t = 0.95$ , green line) and the selection oracle for accepting or rejecting corrections using each method. Guided proofreading yields better results faster with fewer corrections.

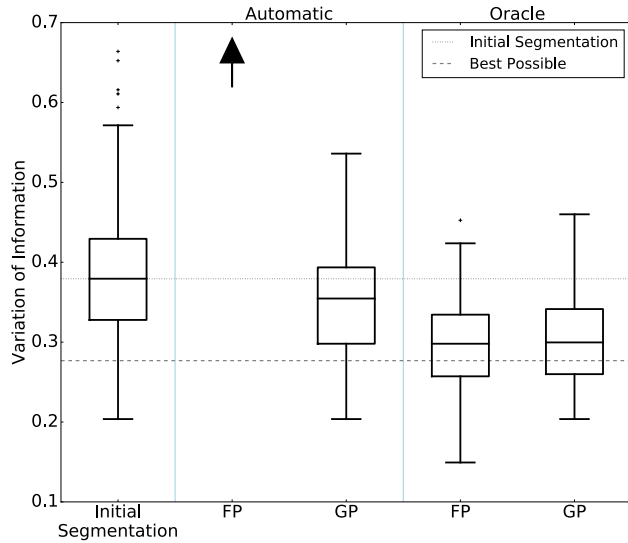


Figure 4: VI distributions of guided proofreading (GP) and focused proofreading (FP) output across slices of the L. Cylinder dataset, with different error correction approaches. The variation resulting from performance of FP with automatic selection is  $7.8 \times$  higher than GP (as indicated by the arrow), with median VI of 2.75 and  $SD = 0.789$ .

voxels. The subvolumes were cut from the last 25 sections of each of the three datasets and unseen during training. We compare focused proofreading and guided proofreading with automatic selection ( $p_t = 0.95$ ) and selection oracle.

**Retraining.** Since the CREMI data is a different species, we simply retrain our split error classifier as well as focused proofreading by Plaza [4]. For this, we use the first 100

sections of each of the three CREMI datasets combined as training data. All parameters are unchanged and left as reported in the paper.

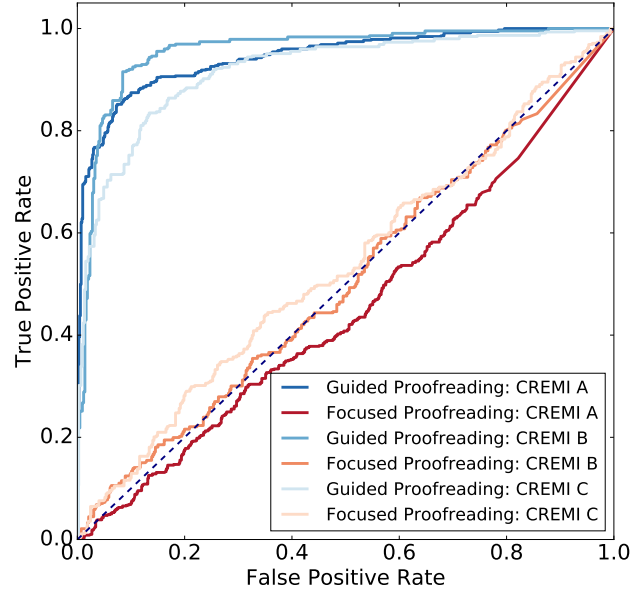


Figure 5: Receiver Operating Characteristic curves comparing focused proofreading and guided proofreading automatic correction on the CREMI A/B/C fruit fly subvolumes. Guided proofreading performs better on all three datasets.

**Classification Performance.** Figure 5 compares the focused proofreading and guided proofreading classifiers on the CREMI A/B/C datasets. Our method exhibits higher sensitivity and lower fall-out.

#### 4.1. CREMI A

Figure 6 and 7 compare Plaza’s focused proofreading and guided proofreading on the 5 sections of the CREMI A dataset.

**Selection oracle.** With focused proofreading, the selection oracle reduces median VI to 0.928,  $SD = 0.043$  from an initial median VI of 1.06 ( $SD = 0.055$ ). 532 corrections out of 3707 were accepted. Guided proofreading does not reach the best possible VI, however, reduces VI faster with less corrections to 0.941 ( $SD = 0.04$ ). Out of 4463 corrections, 1275 were accepted.

**Automatic selection with threshold.** Not surprisingly, focused proofreading performs poorly when ran automatically (VI of 5.32,  $SD = 0.009$ ). Guided proofreading is able to reduce VI to 0.989 ( $SD = 0.043$ ) with  $p_t = 0.95$ .

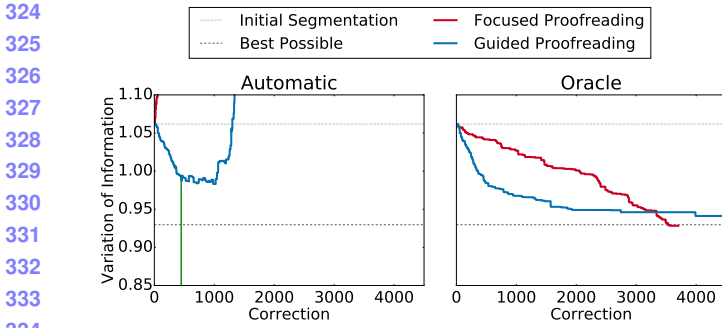


Figure 6: Performance comparison of Plaza’s focused proofreading and our guided proofreading on 5 sections of the CREMI A dataset. All measurements are reported as median VI, the lower the better. The threshold for automatic selection is  $p_t = 0.95$  (green line). The slope of the selection oracle shows that guided proofreading reduces VI faster.

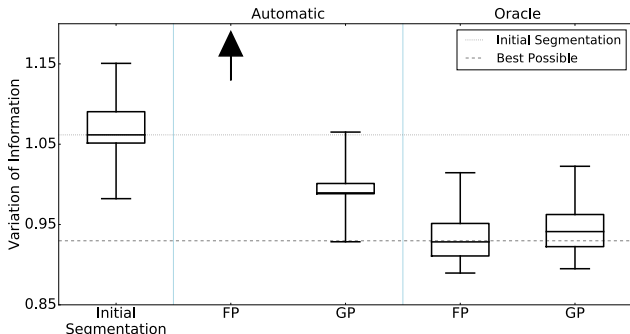


Figure 7: VI distributions of guided proofreading (GP) and focused proofreading (FP) output across slices of the CREMI A dataset, with different error correction approaches. The variation resulting from performance of FP with automatic selection is  $5.4 \times$  higher than GP (as indicated by the arrow), with median VI of 5.32 and  $SD = 0.009$ . GP does not reach the best possible VI as discussed in the text.

## 4.2. CREMI B

Figure 8 and 9 show the results on the CREMI B dataset.

**Selection oracle.** Focused proofreading is able to reduce median VI to 1.29,  $SD = 0.031$  from an initial median VI of 1.63 ( $SD = 0.025$ ). Out of 1959 corrections, the selection oracle accepted 517. With guided proofreading, the median VI is reduced to 1.30,  $SD = 0.03$  while accepting 1111 corrections out of 3073.

**Automatic selection with threshold.** Focused proofreading results in a VI of 4.25 ( $SD = 0.07$ ). Guided proofreading reduces median VI to 1.43 ( $SD = 0.038$ ).

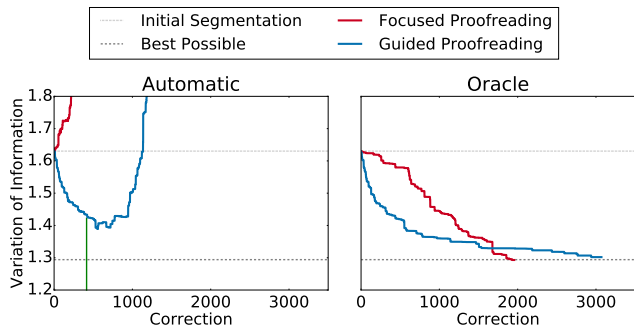


Figure 8: Split error correction by Plaza’s focused proofreading and our guided proofreading compared on the CREMI B dataset. All measurements are reported as median VI, the lower the better. Automatic selection with threshold (green line) yields reasonable performance using guided proofreading.

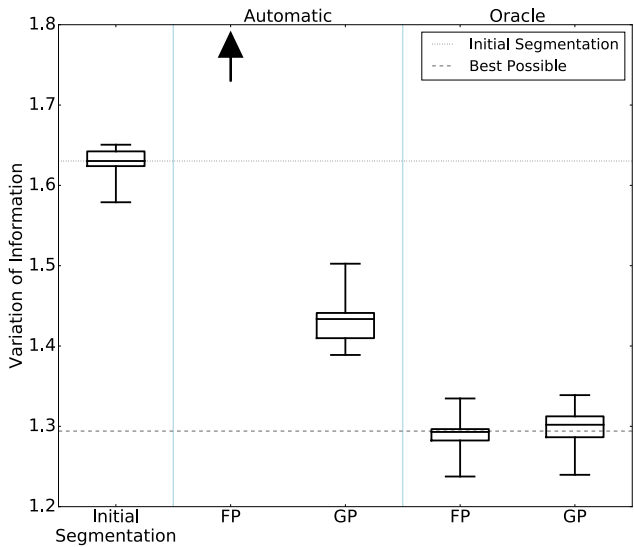


Figure 9: VI distributions of guided proofreading (GP) and focused proofreading (FP) output across 5 sections of the CREMI B dataset. We compare automatic selection and oracle selection. The variation resulting from performance of FP with automatic selection is  $3 \times$  higher than GP (as indicated by the arrow), with median VI of 4.25 and  $SD = 0.07$ .

## 4.3. CREMI C

The results of split error correction using focused proofreading and guided proofreading on the CREMI C subvolume are shown in Figure 10 and 11.

**Selection oracle.** With focused proofreading, the initial median VI of 1.75 ( $SD = 0.086$ ) is reduced to 1.45 ( $SD = 0.056$ ) with 670 accepted corrections out of 2694. Guided

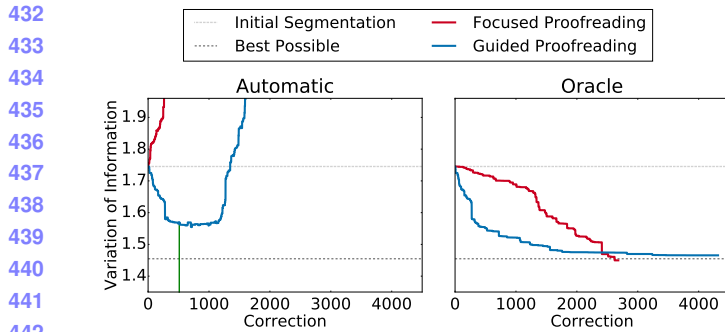


Figure 10: Performance comparison of Plaza’s focused proofreading and our guided proofreading on the CREMI C dataset. Lower VI scores are better. Guided proofreading corrects the initial segmentation faster with less corrections than focused proofreading. The green line shows the automatic threshold  $p_t = 0.95$ .

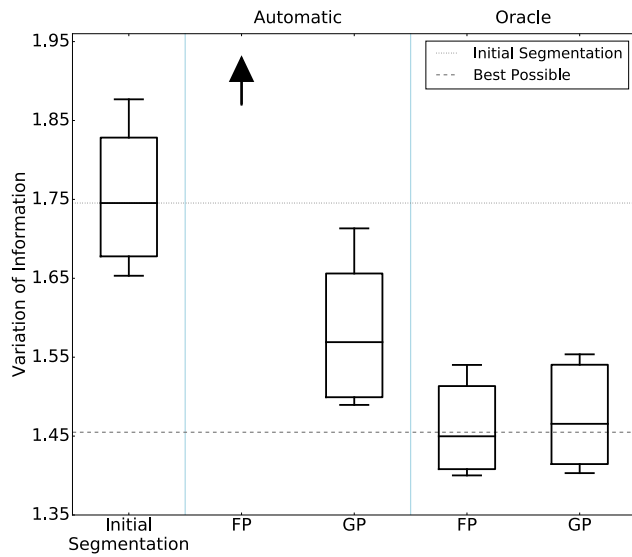


Figure 11: VI distributions of guided proofreading (GP) and focused proofreading (FP) output across the CREMI C subvolume, with different error correction approaches. The variation resulting from performance of FP with automatic selection is 3× higher than GP (as indicated by the arrow), with median VI of 4.81 and  $SD = 0.08$ .

proofreading is able to reduce the VI to 1.47 ( $SD = 0.06$ ). Here, the oracle accepted 1531 out of 4332 corrections.

**Automatic selection with threshold.** Focused proofreading results in a VI of 4.81 ( $SD = 0.03$ ). Guided proofreading with  $p_t = 0.95$  reduces median VI to 1.57 ( $SD = 0.081$ ).



Get **\$10** Cash!  
And look at

## Pretty Pictures of the brain while helping to Advance Science

We are looking for people who are 18+ and have no experience with nano-scale electron microscopy data of neurons (noobs).

The experiment will last less than 1 hour.

Starting NOW!

SIGN UP:  
<http://XXX/YYXXXXXXZZZZ>

Contact: Anon. <[anon@anon](mailto:anon@anon)>  
Anon.

Figure 12: Participants were recruited with this flyer.

## 5. Forced Choice User Experiment

### 5.1. Recruitment and Participation

Novice participants were recruited via flyer (figure 12). An anonymized listing of all participants including demographic information is shown in table 4.

### 5.2. Example Classifications

During the user study, participants were asked to accept or reject potential errors and their corrections — some more difficult than others. Figure 14 shows a selection of potential errors and their corrections.

### 5.3. Subjective Responses

After the experiment, we acquired subjective responses using the NASA-TLX task load index (figure 13). We performed ANOVA to test for statistical significance [6]. Mental, physical, and temporal demands were reported slightly higher for participants using focused proofreading but the analysis did not yield any significance.

- **Mental Demand.** Participants using focused proofreading stated a higher mental demand  $M = 11.5$  ( $SD = 2.098$ ) than with guided proofreading  $M = 8.1$

540

**NASA Task Load Index**

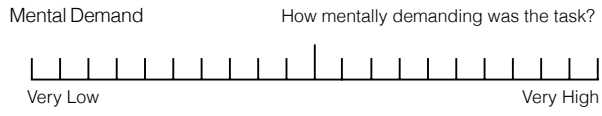
541

Hart and Staveland's NASA Task Load Index (TLX) method assesses work load on five 7-point scales. Increments of high, medium and low estimates for each point result in 21 gradations on the scales.

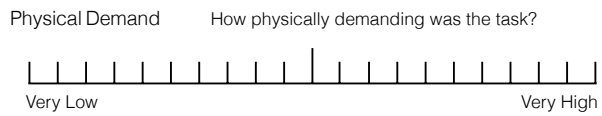
545

Name	Task	Date
------	------	------

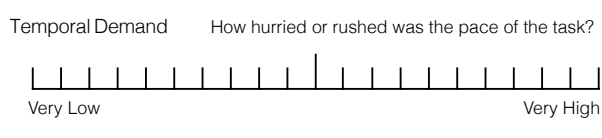
546



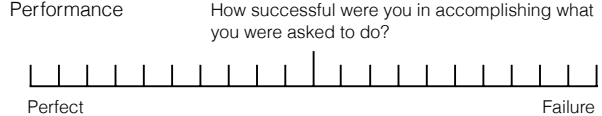
547



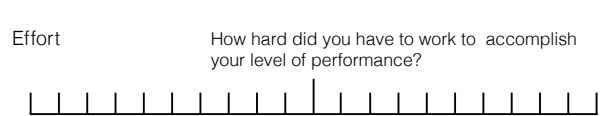
548



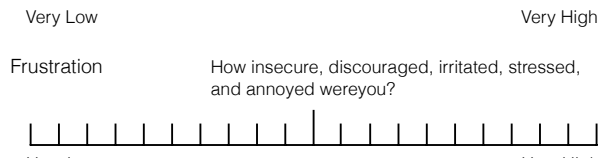
549



550



551



552

Figure 13: The NASA-TLX workload index to record subjective responses.

557

( $SD = 2.003$ ). This was not statistically significant ( $F_{1,18} = 3.2574, p = 0.3695$ ).

558

- **Physical Demand.** While naturally physical demand was rated low, participants using focused proofreading stated it slightly higher  $M = 5.4$  ( $SD = 2.26$ ) than with guided proofreading  $M = 2.9$  ( $SD = 1.76$ ). This was not statistically significant ( $F_{1,18} = 1.7507, p = 0.5454$ ).

559

- **Temporal Demand.** For temporal demand, participants using focused proofreading  $M = 8.4$  ( $SD = 1.95$ ) reported almost equal to guided proofreading  $M = 8.3$  ( $SD = 1.99$ ). This was not statistically significant ( $F_{1,18} = 0.0033, p = 0.9987$ ).

560

- **Performance.** Here, participants were asked to rate

ID	Sex	Age	Classifier
S38	F	20	FP
S57	F	30	FP
S32	M	38	FP
S34	F	21	FP
S21	F	65	FP
S9	M	33	FP
S45	M	28	FP
S31	M	27	FP
S24	F	21	FP
S6	F	38	FP
S28	M	32	GP
S36	F	19	GP
S35	M	26	GP
S25	M	26	GP
S54	F	30	GP
S53	M	29	GP
S52	M	27	GP
S51	M	31	GP
S200	F	37	GP
S3	F	30	GP

Table 4: The novice participants ( $N = 20$ ) of the forced choice user experiment. The table shows sex (20 female), age ( $M = 30$ ) and the randomly assigned classifier (focused proofreading as FP, guided proofreading as GP).

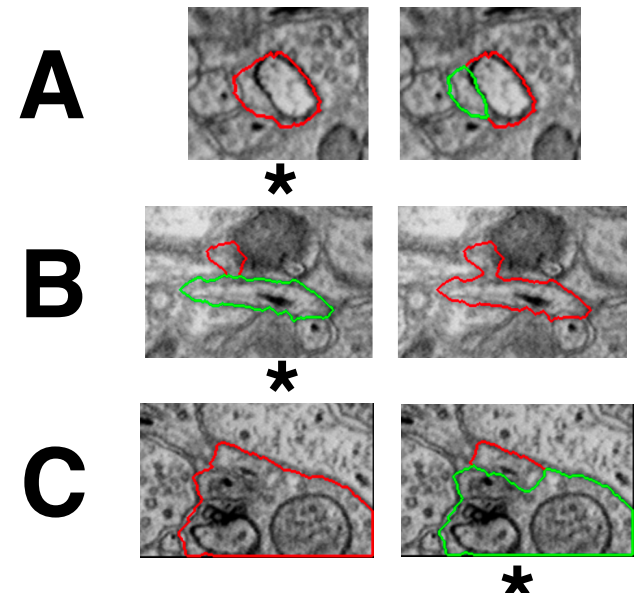


Figure 14: A selection of suggested errors and potential corrections during the forced choice user experiment. The star (\*) indicates which choice reduces VI. While all participants were able to correctly choose for patch A, only few were able to correctly choose for patch B and C.

648 their own performance. All participants rated their  
649 performance as pretty well (the lower, the better). For  
650 focused proofreading  $M = 6.8$  ( $SD = 1.97$ ) and for  
651 guided proofreading  $M = 7.8$  ( $SD = 2.04$ ). This  
652 was not statistically significant ( $F_{1,18} = 0.3091, p =$   
653 0.8878).  
654

655 • **Effort.** Participants using focused proofreading stated  
656 higher effort  $M = 13.0$  ( $SD = 2.336$ ) than with  
657 guided proofreading  $M = 10.6$  ( $SD = 2.127$ ). This  
658 was not statistically significant ( $F_{1,18} = 1.1459, p =$   
659 0.6599).

660 • **Frustration.** Participants overall reported low frustration.  
661 Reported were  $M = 5.0$  ( $SD = 1.90$ ) using  
662 focused proofreading and  $M = 5.9$  ( $SD = 1.85$ ) using  
663 guided proofreading. This was not statistically signifi-  
664 cant ( $F_{1,18} = 0.3271, p = 0.8818$ ).  
665

## 666 References 667

- [1] K. He, X. Zhang, S. Ren, and J. Sun. Deep residual learning  
668 for image recognition. In *The IEEE Conference on Computer  
669 Vision and Pattern Recognition (CVPR)*, June 2016. 1  
670
- [2] S. Knowles-Barley, V. Kaynig, T. R. Jones, A. Wilson, J. Morgan,  
671 D. Lee, D. Berger, N. Kasthuri, J. W. Lichtman, and  
672 H. Pfister. Rhoanet pipeline: Dense automatic neural anno-  
673 tation, 2016. (available on arXiv:1611.06973 [cs.CV]). 2  
674
- [3] J. Nunez-Iglesias, R. Kennedy, S. M. Plaza, A. Chakraborty,  
675 and W. T. Katz. Graph-based active learning of agglomeration  
676 (gala): a python library to segment 2d and 3d neuroimages.  
677 *Frontiers in neuroinformatics*, 8, 2014. 2  
678
- [4] S. M. Plaza. *Focused Proofreading to Reconstruct Neural Con-*  
679 *nnectomes from EM Images at Scale*, pages 249–258. Springer  
680 International Publishing, Cham, 2016. 3  
681
- [5] O. Ronneberger, P. Fischer, and T. Brox. U-net: Convolutional  
682 networks for biomedical image segmentation. In *Medical Im-*  
683 *age Computing and Computer-Assisted Intervention (MICCAI)*,  
684 volume 9351 of *LNCS*, pages 234–241. Springer, 2015. (avail-  
685 able on arXiv:1505.04597 [cs.CV]). 2  
686
- [6] J. P. Shaffer. Multiple hypothesis testing. *Annual Review of*  
687 *Psychology*, 46(1):561–584, 1995. 5  
688

689  
690  
691  
692  
693  
694  
695  
696  
697  
698  
699  
700  
701

702  
703  
704  
705  
706  
707  
708  
709  
710  
711  
712  
713  
714  
715  
716  
717  
718  
719  
720  
721  
722  
723  
724  
725  
726  
727  
728  
729  
730  
731  
732  
733  
734  
735  
736  
737  
738  
739  
740  
741  
742  
743  
744  
745  
746  
747  
748  
749  
750  
751  
752  
753  
754  
755